Published in final edited form as:
IEEE Trans Neural Syst Rehabil Eng. 2012 July ; 20(4): 422–431. doi:10.1109/TNSRE.2012.2197865.

Toward a noninvasive automatic seizure control system in rats with transcranial focal stimulations via tripolar concentric ring electrodes

Oleksandr Makeyev [Member, IEEE]
Department of Electrical, Computer, and Biomedical Engineering, University of Rhode Island, Kingston, RI 02881, USA

Xiang Liu [Student Member, IEEE]
Department of Electrical, Computer, and Biomedical Engineering, University of Rhode Island, Kingston, RI 02881, USA

Hiram Luna-Munguía [Member, IEEE]
Department of Electrical, Computer, and Biomedical Engineering, University of Rhode Island, Kingston, RI 02881, USA

Gabriela Rogel-Salazar
Department of Electrical, Computer, and Biomedical Engineering, University of Rhode Island, Kingston, RI 02881, USA

Samuel Mucio-Ramirez
Departamento de Neuromorfologia Funcional, Instituto Nacional de Psiquiatria Ramon de La Fuente Muñiz, Mexico 14370, Mexico (mucios@yahoo.com)

Yuhong Liu [Student Member, IEEE]
Department of Electrical, Computer, and Biomedical Engineering, University of Rhode Island, Kingston, RI 02881, USA

Yan L. Sun [Member, IEEE]
Department of Electrical, Computer, and Biomedical Engineering, University of Rhode Island, Kingston, RI 02881, USA

Steven M. Kay [Fellow, IEEE]
Department of Electrical, Computer, and Biomedical Engineering, University of Rhode Island, Kingston, RI 02881, USA

Walter G. Besio [Senior Member, IEEE]
Department of Electrical, Computer, and Biomedical Engineering, University of Rhode Island, Kingston, RI 02881, USA

Abstract

Epilepsy affects approximately one percent of the world population. Antiepileptic drugs are ineffective in approximately 30% of patients and have side effects. We are developing a noninvasive, or minimally invasive, transcranial focal electrical stimulation system through our novel tripolar concentric ring electrodes to control seizures. In this study we demonstrate feasibility of an automatic seizure control system in rats with pentylenetetrazole-induced seizures through single and multiple stimulations. These stimulations are automatically triggered by a real-

phone: 401-874-4738; fax: 401-872-6422; omakeyev@ele.uri.edu, liu@ele.uri.edu, hiram_luna@yahoo.com, gaby.rogel@gmail.com, yuhong@ele.uri.edu, yansun@ele.uri.edu, kay@ele.uri.edu, besio@ele.uri.edu

time electrographic seizure activity detector based on a disjunctive combination of detections from a cumulative sum algorithm and a generalized likelihood ratio test. An average seizure onset detection accuracy of 76.14% was obtained for the test set (n = 13). Detection of electrographic seizure activity was accomplished in advance of the early behavioral seizure activity in 76.92% of the cases. Automatically triggered stimulation significantly ($p = 0.001$) reduced the electrographic seizure activity power in the once stimulated group compared to controls in 70% of the cases. To the best of our knowledge this is the first closed-loop automatic seizure control system based on noninvasive electrical brain stimulation using tripolar concentric ring electrode electrographic seizure activity as feedback.

Keywords

brain stimulation; electrographic seizure feedback control; transcranial focal stimulation; tripolar concentric ring electrodes; seizure detection

I. Introduction

EPILEPSY is a neurological disorder that affects approximately one percent of the world population with up to three-fourths of all people with epilepsy living in developing countries [1]. Anti-epileptic drugs are ineffective in up to 30% of patients and can cause side effects [2]. Surgery is another option available, but carries risks [3].

Recently electrical stimulation of the brain has shown promise in reducing seizure frequency. Implantable techniques such as the deep brain stimulation [4–8], the responsive neurostimulator [9, 10], and the vagus nerve stimulation [11–15] have been widely studied. Noninvasive forms of brain stimulation for epilepsy are gaining acceptance. There is a growing body of research on different forms of noninvasive electrical stimulation including transcranial magnetic stimulation [16–19] and transcranial direct current stimulation (tDCS) [20]. Yet, as previously concluded by Theodore and Fisher in a review of various brain stimulation techniques, the best structures to stimulate and the most effective stimuli to use are still unknown [21].

Concentric ring electrodes (CREs) have unique capabilities. They perform the second spatial derivative, the Laplacian, on the surface potentials. Previously we have shown that tEEG, Laplacian electroencephalography (EEG) with the tripolar concentric ring electrode (TCRE) configuration, is superior to conventional EEG with disc electrodes since tEEG has significantly better spatial selectivity, signal-to-noise ratio, localization, approximation of the analytical Laplacian, and mutual information [22–24]. These findings suggest that tEEG may be superior at detecting seizures, or other neurological disorders, to conventional EEG with disc electrodes.

Unlike electrical stimulation via conventional disc electrodes that is usually applied across the head, transcranial electrical stimulation via CRE has a much more uniform current density [25] and focuses the stimulation directly below the electrodes. Therefore, we call this form of stimulation transcranial focal stimulation (TFS).

Promising results using TFS to attenuate acute seizures in a pilocarpine-induced status epilepticus model have been previously achieved by our group [26] where TFS via TCRE attenuated electrographic seizure activity toward baseline and halted the progression of behavioral seizures. Moreover, interruption of the seizure activity appeared to be a long-lasting effect and the TFS treatment significantly enhanced the survival of rats after status

epilepticus. We have also shown that TFS, after severe penicillin-induced [27] myoclonic jerks (MJs), significantly decreased MJs in number and duration.

To further validate the effect of the TFS, it was used in a third animal model, the pentylenetetrazole (PTZ) model, widely used for testing both seizure susceptibility and screening of new antiepileptic drugs [28]. As a first step, the potential of TFS to reduce pathological synchronization of PTZ-induced electrographic activity was studied [29]. Cross-channel coherence was used to measure synchrony changes at particular frequency bands in electrographic activity recorded from TCREs on the rat scalp. Cross-channel coherence was performed on tEEG segments recorded (a) during the preseizure stage, (b) after administration of PTZ, and (c) immediately after application of TFS. A significant increase in synchrony within the beta-gamma frequency bands during seizures was demonstrated as well as the potential of TFS to significantly reduce this synchrony.

As we continued using TFS via TCREs on the scalp of rats after PTZ induced seizures we found TFS caused reductions of both seizure electrographic activity power for 4 min long time windows starting after the TFS treatment [30] and duration of myoclonic activity [31]. Finally, in [32] a cumulative sum (CUSUM) seizure detecting algorithm was proposed to trigger automatic application of TFS. The CUSUM algorithm was evaluated on pre-recorded data and detected the electrographic seizure activity in all experiments well in advance of the behavioral seizure activity.

An important advantage of TFS is that it does not cause motor contractions as is common with electroconvulsive therapy, another form of transcranial electrical stimulation. The rats do not show signs of pain or aversion when TFS is applied via TCRE and continue to roam freely. The effects of TFS via CRE on rat skin were quantitatively analyzed in [33] through calculation of the temperature profile under the CRE and corresponding energy density with electrical-thermal coupled field analysis using a three-dimensional multi-layer model. Infrared thermography was also used to measure skin temperature during electrical stimulation to verify the computer simulations. Histological analysis was performed to study cell morphology and characterize any resulting tissue damage. It was concluded that as long as the specified energy density applied through the CRE was kept below 0.92 (A^2/cm^4s^{-1}), the maximum temperature remained within the safe limits and also within the limits of the melting point of conductive paste and provided a safe current density distribution. Effects of TFS via TCRE on rat cortical integrity were studied in [34]. Histomorphological analysis was used to assess cortical areas below the TFS site for neuronal damage. Control and TFS treated animals were anaesthetized and transcardially perfused. The brains were removed, post-fixed, and cut into coronal sections. Slices were mounted on gelatinized slides, Nissl stained for brightfield analysis, and photographed with a microscope equipped with a digital camera. Images where digitized to grayscale and the integrated optical density was measured with densitometry software. No significant difference in integrated optical density was found for control and TFS treated rat brains and morphological analysis did not show any pyknotic neurons, cell loss or gliosis that might confirm any neuronal damage.

As the next fundamental step in this study we attempt to close the loop showing feasibility of an automatic seizure control system in rats with PTZ-induced seizures through single and multiple applications of TFS via TCRE. TFS is automatically triggered by real-time electrographic seizure activity detectors based on a disjunctive combination of the CUSUM algorithm and generalized likelihood ratio test (GLRT). We performed experiments following the methodology proposed in [30] and [32] to confirm the effect of automatically triggered TFS on PTZ-induced electrographic seizure activity in rats.

Recently many studies have been performed in the field of seizure detection [35–37]. In our case the most relevant are recent studies on PTZ-induced seizure onset detection in rats [38–40]. Actually, in previous works [30, 32] we had found a significant increase in tEEG power corresponding to seizure onset using population grand average power spectral density estimates and frequency band analysis. These findings agree well to findings of others where power related features were used as features for seizure detection including variance energy in [39] and signal and wavelet energy in [40]. Based on these findings the seizure onset detection methodology proposed in this paper is based on detecting the changes in signal power.

Detection of seizures is challenging because: (1) there is no objective definition of what constitutes seizure electrographic activity, (2) background brain activity is non-stationary, (3) the changes introduced by seizures are non-stationary, (4) movement artifacts or non-seizure activity of the brain may resemble seizure activity, and (5) early detection, with high accuracy and specificity are required.

The CUSUM is a signal change detector traditionally used in quality control, intrusion detection, spam filtering and medical systems to identify changes in probability distribution of a stochastic random process. The CUSUM was selected because it is able to rapidly and reliably detect small changes and is insensitive to the probability distribution of the data [41].

Although there is no optimality associated with the GLRT it has been shown to work well in practice [42]. Moreover, asymptotically, it was shown that the GLRT is a uniformly most powerful test among tests that are invariant, i.e. among all possible invariant tests that have a given probability of false alarm it gives the highest probability of detection [43].

II. Methods

A. Animals

Sprague-Dawley rats (220 ′ 320 g body weight) maintained under environmentally controlled conditions (12 h normal light/dark cycles, 25°C) with food and water ad libitum, were used in the present study. The experimental protocol was approved by the University of Rhode Island IACUC.

B. Electrodes Attachment

Rats were anesthetized with a mixture of ketamine (80 mg/kg) and xylazine (12 mg/kg) i.p. Then, the scalp of the rat was shaved and prepared with NuPrep abrasive gel (D. O. Weaver & Co., Aurora, CO, USA). Three custom-designed TCREs [22] were implanted on the rat scalp using conductive paste (0.5 mm Ten20, Grass Technologies, RI, USA) and fixed to it with dental acrylic (Pearson Lab Supply, Sylmar, CA, USA).

As shown in Fig. 1 one TCRE (diameter = 1.0 cm), was used to record and stimulate and was centered on the top of the head (1). The front edge of the electrode was placed near the site that should be the bregma since we were not able to see it. Two other TCREs (diameter = 0.6 cm) were placed bilaterally behind the eyes, but in front of the ears (A 2.0 mm, L 9.0 mm relative to the central electrode) on both sides of the head (2,3). An isolated ground electrode was attached on the top of the neck behind the ears (g). These particular electrode locations were chosen due to size constraints and brain anatomy of adult rats. The rat was returned to its cage and allowed food and water ad libitum for approximately 24 h until the experimental procedure began. All experiments were performed in the afternoon.

C. Experimental Procedure

The day of the experiment, the rats were allowed to habituate to the room and the electrode cables for approximately 30 min. First, the skin-to-electrode impedance of each electrode was measured. If the outer ring or central disc skin-to-electrode impedance for the 1.0 cm dia. electrode (1) to the isolated ground electrode (g) of Fig. 1 was less than 10 KΩ, then the rat was given TFS once or twice. If this impedance was greater than 10 KΩ, but less than 25 KΩ and impedance for at least one of the 0.6 cm dia. electrodes (2) and (3) to the isolated ground electrode (g) was less than 20 KΩ then the rat was assigned to the control group. Lower impedances for electrode (1) for TFS treated group ensured effectiveness of TFS. The skin-to-electrode impedance was rechecked at the end of the experiment.

Next, the tEEG recording and the video recording were started. To evaluate the accuracy of the seizure detection data were collected for each rat in the following way: first, 5 min of baseline tEEG were recorded to train the seizure detector. Next, the seizure detector was activated for 5 min of sham seizure activity (baseline) recording. Finally, seizures were induced with PTZ (55 mg/kg i.p.) and the tEEG recording continued for another 15 min. In the TFS-treated groups one or two doses of TFS were automatically triggered (300 Hz, 50 mA, 200 μs, biphasic square pulses for 2 minutes) and administered between the outer ring and the central disc of electrode (1). The TFS pulses were generated by a custom-built stimulator that was controlled with a BS2P-24 microcontroller (Parallax Inc., CA, USA).

D. Signal Acquisition and Preprocessing

The tEEG signals were preamplified (gain 100 and 0.3 Hz high pass filter) with a custom built preamplifier and then amplified using a Grass Model NRS2 Neurological Research System with Model 15A54 AC amplifiers (Grass Technologies, West Warwick, RI, USA) with a gain of 1000 and band pass of 1.0–100 Hz with the 60 Hz notch filter active, and digitized (16 bits, 256 Hz). Two differential signals from each electrode were combined with an algorithm to give Laplacian derivation of the signal as reported previously in [22]. Briefly, the algorithm is two-dimensional and weights the middle ring and central disc difference sixteen times greater than the outer ring and central disc difference.

For automatic seizure onset detection data recorded from electrode (1) was used for TFS treated rats while data from the electrode with the lowest impedance was used for the control group. This was done to ensure the highest possible quality of the tEEG signal for all the groups. For assessing the effect of TFS on electrographic seizure activity power data recorded from electrode (1) was used for both TFS treated and control groups to compensate for potential difference in power between electrodes differing in size and/or location. Such a difference is not crucial for automatic seizure onset detection due to the fact that individual detection models were used for each rat. Real-time signal acquisition and processing as well as post signal processing was performed using Matlab (Mathworks, Natick, MA, USA).

E. Automatic Seizure Onset Detection

Detection Model and Dataset—We tested three seizure detectors in this study (1) supervised CUSUM, and two implementations of GLRT: supervised and unsupervised (further termed (2) sGLRT and (3) uGLRT respectively). For CUSUM and sGLRT we used individualized models of the real-time seizure onset detection i.e. the detector was trained on baseline electrographic activity for each rat. For the uGLRT model there was no training performed on data from individual rats. Detection accuracy was calculated for separate detectors as well as their combination. A disjunctive (logical OR) detector fusion rule was used for combining the detector outputs. That is, a detection from either one of the three individual detectors occurring more than 15 s after the PTZ injection triggering TFS in real time. The handling period of 15 s was introduced to avoid movement artifacts, caused by

handling of the rat related to the PTZ injection, from influencing the seizure onset detection. For the two-dose TFS treated group a 45 s delay in triggering the second TFS dose was introduced after ending the first TFS dose to allow recovery of the amplifiers and assure valid tEEG signals.

All the data collected during this study was divided into two datasets. First, the training dataset was collected comprising data from 3 rats, 2 controls and 1 single TFS treated rat. It was used to test the real-time seizure onset detection hardware and software and, more importantly, to determine the suboptimal parameter values for both sGLRT and uGLRT through grid search using the recorded data. The parameter values were selected using a receiver operating characteristic curve based on the tradeoff between maximizing the number of true detections and minimizing the number of false alarms. Suboptimal parameter values for CUSUM were adapted from [32] where they were determined using a similar approach. The test dataset consisted of data from a total of 13 rats: 5 controls, 5 rats treated with a single dose of TFS and 3 rats that received two doses of TFS.

A brief description of CUSUM and GLRT and details of their implementation for seizure onset detection are presented next followed by the performance metrics used.

CUSUM—A detailed derivation of the properties of CUSUM is outside of the scope of this paper and can be found in [32]. We apply CUSUM simultaneously to power in two frequency bands: delta (1 – 4 Hz) and theta (5 – 8 Hz). These specific frequency bands were adapted from our previous study in which they were found to yield the highest detection rates in a non-real-time seizure detection model on pre-recorded data [32]. First, as soon as the 5 min of baseline (pre-seizure) activity are recorded the average baseline power μ_0 is calculated for each of the two frequency bands. The baseline activity is divided into non-overlapping segments of data (epochs). A Hanning window was applied to each epoch and the power spectrum was calculated using Fast Fourier Transform. For each of the two frequency bands the spectrum was summed over frequencies and normalized by the maximum component. Average power of all the epochs of the baseline activity in each frequency band was used as μ_0.

After that, during sham and real seizure detection epochs were acquired in real time. The same processing method used for baseline was also used to calculate the detection function g_k:

$$g_k = \max\left(g_{k-1} + \left(x(k) - \mu_0 - s\right), 0\right)$$

where $x(k)$ is the power of the k-th detection epoch and s is a parameter of the CUSUM detector utilized to adjust the detection sensitivity. An epoch was marked as seizure if and only if the value of the detection function (i.e. g_k) was larger than the threshold $\bar{h}$ for both frequency bands. Other suboptimal CUSUM parameter values were adapted from the same study [32]. Namely, the size of the decision epoch was equal to 1 s, $\bar{h} = \mu_0$ and $s = 0.1$. Finally, to increase the likelihood that we discriminated seizure from movement artifact we implemented a two-of-three `seizure' smoothing algorithm for each band. If two out of three consecutive detection epochs were marked by the CUSUM detector as `seizure' the second `seizure' was considered as a possible seizure onset. If two of three `seizure' were detected in both bands then this was the seizure onset. We reasoned that the seizure activity would be prolonged bursts of activity and the movement artifacts would be shorter in duration.

Generalized Likelihood Ratio Test—A detailed derivation of the properties of GLRT is outside of the scope of this paper and can be found in [42]. We apply GLRT to verify the

change in power between two data segments $x_a(k)$ and $x_b(k)$ ($k = 1,..,N$) of equal size N of white Gaussian noise (WGN) with unknown variances σ_a^2 and σ_b^2 respectively: $x_a(k) \sim N(0, \sigma_a^2)$ and $x_b(k) \sim N(0,\sigma_b^2)$. An overview of GLRT performance for this case is presented next.

We need to test if $\sigma_a^2<\sigma_b^2$ (due to zero mean the power is equal to the variance [44]) so under the null hypothesis $H_0 : \sigma_a^2=\sigma_b^2$ with the alternative being $H_1 :\sigma_a^2<\sigma_b^2$. It can be shown that for this case GLRT decides H_1 if:

$$T(x) = 2N\ln\frac{\frac{1}{2}\sum_{0}^{N-1}\left(x_a^2(k)+x_b^2(k)\right)}{\sqrt{\sum_{0}^{N-1}x_a^2(k)\sum_{0}^{N-1}x_b^2(k)}} > \gamma$$

where $T(x)$ is the test statistic and γ is the test threshold. From the asymptotic performance of $T(x)$ γ can be derived as a function of p value (also called probability of false alarm):

$$\gamma = \left(Q^{-1}\left(\frac{1}{2}p\right)\right)^2$$

where Q^{-1} is the inverse of the complementary cumulative distribution function also referred to as the right-tail probability of Gaussian distribution.

In our study we used sGLRT and uGLRT implementations for seizure detection. The main difference was in selection of data segments x_a and x_b. For uGLRT, both data segments were taken as non-overlapping segments from the data acquired in real time and were adjacent to each other with x_a immediately preceding x_b. In this way the GLRT was detecting a sudden significant increase in power in consecutive segments of data. For sGLRT x_a was selected from baseline tEEG while x_b was taken from sham and real seizure data (data after the PTZ injection) acquired in real time. The following rule was used to select x_a : it was selected as one of the non-overlapping baseline segments of size equal to the size of the detection epoch with power closest to the power of the whole baseline segment multiplied by a scaling factor $\alpha>1$. In this way x_a represents the scaled baseline power while having the size of the detection epoch as required by GLRT. In both cases for each extracted segment the mean was subtracted to comply with the assumption of WGN.

Suboptimal values for GLRT parameters were selected from the training dataset through grid search. A p value equal to 0.05 and 5 sec detection epoch were selected for both sGLRT and uGLRT implementations. The scaling factor α equal to 1.5 was determined for sGLRT in the same way. Finally, to increase the likelihood that we discriminated seizure from movement artifact we implemented a three-of-three `seizure' smoothing algorithm for both implementations. If three consecutive detection epochs were marked by the sGLRT or uGLRT detectors as seizure the third epoch was considered the seizure onset.

Performance Metrics—Seizure onset detection accuracy was calculated for periods of sham and real seizure until the first observed MJ with the exception of a 30 s handling period centered at the moment of PTZ injection. The first MJ was used as an ending point for seizure onset detection accuracy since it is a clear behavioral manifestation of the seizure activity and for our seizure control we would prefer to detect the seizure before the physical

behavioral activity. The actual duration of the seizure segment used to evaluate detection accuracy varied greatly as some rats showed delayed onset of their first MJ until after the recording was finished. In those cases the end of the recording served as the ending of seizure segment for evaluation of detection accuracy. The rats with long latency distorted the average latency of the first MJ for the test dataset (231.8±356.6 s) while the median of 59 s is more accurate.

For each detection method, or a disjunctive combination of methods, the automatically detected seizure score was compared with the gold standard score. For the automatic score each detection epoch was marked as either presence or absence of seizure. For the gold standard every detection epoch belonging to the period starting with the beginning of sham seizure and ending 15 s before the PTZ injection was marked as absence of seizure while every epoch belonging to the period starting 15 s after PTZ injection and ending at the first MJ was marked as seizure.

Since the size of the detection epoch for CUSUM was different from the detection epoch for sGLRT and uGLRT (1 s and 5 s correspondingly) they had to be unified for calculation of seizure detection accuracy. Five second long epochs were used for all three methods with the CUSUM epoch marked as seizure if at least one of 1 s subepochs was marked as seizure by the detector.

The accuracy was calculated by identifying all situations where either automatic or gold standard scores indicated presence of seizure and calculating the numbers of true positives (T_+), true negatives (T_-), false positives (F_+) and false negatives (F_-) in terms of 5 s epochs. These detections were later used to calculate sensitivity $\left(\frac{T_+}{T_+ + F_-}\right)$ and specificity $\left(\frac{T_-}{T_- + F_+}\right)$ to further calculate the overall accuracy $\left(\frac{T_+ + T_-}{T_+ + T_- + F_+ + F_-}\right)$ as a weighted average of sensitivity an specificity [45].

Electrographic Seizure Activity—For this part of the study GLRT was used to compare the average power of electrographic seizure activity for the single dose TFS treated and control rats. Since the sizes of data segments x_a and x_b being compared have to be equal for GLRT, the duration of all the segments were set equal to the minimum available data duration from the beginning of the segment to the end of the recording for all the rats. Three and a half minutes long segments were selected for each rat starting 4 min after the first valid seizure detection. The 4 min accounted for the duration of TFS for treated rats, full recovery of amplifiers after application of the TFS dose and time needed to turn the TFS on and off.

In our previous study [30] analysis of grand average power spectral densities was performed to compare different stages of seizure development. It showed a significant difference between the TFS treated group and the control group. In the TFS treated group, after TFS, the power spectral density was reduced further towards a pre-seizure “baseline” than it was for the control group. The difference was most obvious in delta (1 – 4 Hz), theta (5 – 8 Hz) and alpha (9 – 13 Hz) frequency bands. Based on these results digital low-pass zero-phase filter (fifth order Butterworth) was applied to data segments x_a and x_b with a cutoff frequency of 15 Hz to emphasize the difference between control and TFS treated groups.

Filtered segments with the mean subtracted were assumed to be WGN with unknown variances. The test hypotheses were defined in the following way: under the null hypothesis powers of two segments corresponding to control (x_b) and TFS treated rats (x_a) were equal, therefore TFS was not effective in changing the power. The alternative being the power for

the segment corresponding to the TFS treated rat is less than the variance for the control rat. The p value was set to 0.001 to ensure significance between the powers from different segments.

III. Results

A. Automatic Seizure Onset Detection

To illustrate our seizure detection approach the normalized tEEG power calculated on per second basis for segments of data from three rats typical for: control (panel A), and one or two doses of TFS treated groups (panels B and C respectively) are presented in Fig. 2. The following parts of the recorded data are presented in the figure for each rat starting from the beginning of the recording: baseline activity (5 min), sham seizure activity (5 min), and real PTZ-induced seizure activity before and after the first MJ. Seizure activity before and after the first MJ are marked differently since the first MJ was used as the end point for seizure onset detection accuracy evaluation. The segments for TFS doses (2 min each) are also marked. The CUSUM, sGLRT and uGLRT individual detections are shown for each rat as well as the valid trigger used to start the TFS dose. For further analysis we refer to the valid trigger detections as seizure onset detections for each detector and the disjunctive combination of detectors.

Average seizure onset detection accuracies, sensitivities and specificities for the test set (n = 13) for three separate detectors and their disjunctive combination are presented in Table 1. Since there were limited false positive detections the specificities for all three detectors are high as can be seen in Fig. 2 for the period of sham seizure activity.

The highest average seizure detection accuracy of 78.31% was obtained for sGLRT. However, the disjunctive combination of all three detectors gave the highest mean (61.72%) of average sensitivity and average specificity. Furthermore, there are three other important factors to take into account when evaluating the seizure onset detection performance. First one is the percentage of rats in the test group where seizure onset was detected prior to the first MJ. For example, in panel B of Fig. 2 the seizure onset was detected 12 seconds after the first MJ. It can be seen from Table 1 that the highest percentage of 76.92% corresponds to the disjunctive combination of all three detectors. Second one is the time between administration of PTZ and detection of seizure onset. From Table 1 the shortest median latency of 18 s corresponds to the disjunctive combination of the three detectors. Finally, the median latency is used in Table 1 instead of mean and standard deviation since the sGLRT, for one of the rats, produced no seizure onset detection. Taking all these factors into account we can conclude that the disjunctive combination of all three detectors showed the best performance compared to individual detectors.

B. Electrographic Seizure Activity

Fig. 2 shows that baseline and sham seizure activity segments of the recordings have the least power. After the administration of PTZ there is an increase in electrographic activity in all three rats shown which is expected since PTZ induces high-frequency electrographic spiking activity. After the application of one or two doses of TFS (panels B and C respectively), the power of electrographic seizure activity reduced further towards the baseline. This is in contrast to the control rat (panel A). For conclusive proof that TFS significantly reduced the power of electrographic seizure activity in the TFS treated group compared to controls the GLRT was used on 3.5 min long segments of data. Data from a total of 5 TFS treated rats (single TFS dose) and 4 controls from the test set were used. The electrode interface cable of fifth control rat of the test set was disconnected by severe movements during PTZ-induced clonic activity with rearing and falling. Therefore, the data

from the fifth control rat had to be excluded from this part of the study. The GLRT was applied to pairs of data segments corresponding to control and single dose TFS treated groups and the results were averaged for all the pairs. The GLRT showed that TFS significantly ($p = 0.001$) reduced the power of the electrographic seizure activity in the single dose TFS treated group compared to controls in 70% of the pairs. The median power for the TFS group was 2.2 times smaller than the one for the control group with average standard errors in both groups being below 8% and 3% of the median power respectively.

IV. Discussion

A. Automatic Seizure Onset Detection

From Table 1 it can be seen that out of three proposed detectors the worst performance has been shown by uGLRT. This is to be expected since it was the only unsupervised detector. Our motivation to include it into this study was an important advantage of unsupervised detectors - they can be applied to the data from a rat the detector has never been trained on.

The performance of two supervised detectors, CUSUM and sGLRT, was comparable in terms of all the performance metrics. The sGLRT performed slightly better especially on sham seizure (specificity of 97.66% compared with 91.9% for CUSUM) as can be seen, for example, in panel C of Fig. 2. This is important since in real life applications a false positive detection may mean an extra dose of electrical stimulation or a dose of anticonvulsant drug. As a result of a tradeoff higher specificities mean lower sensitivities but even with the sensitivity of 33.73% for a disjunctive combination of all three detectors the seizure onset was detected prior to the first MJ in 76.92% of rats of the test set (n = 13). At the same time disadvantages of sGLRT compared to CUSUM include a much larger detection epoch (5 s compared with 1 s for CUSUM) and the fact that it was the only detector that failed to detect seizure onset in one of the rats completely.

Since all of the proposed detectors are detecting an increase in tEEG power the strong movement artifacts pose a risk of causing false positive detections. One example of such an artifact that was observed to cause false positive detections during the data collection was when a rat was grooming with the paws touching the head electrode cap and connector cables. Artifacts occurring during the baseline part of the recording also pose a threat as the performance of supervised seizure detectors such as CUSUM and sGLRT rely on baseline power of a particular rat. Higher power of the baseline signal due to multiple artifacts increases the detection threshold causing false negative detections and therefore lowering the sensitivity.

Another important consideration is the second TFS trigger seizure detection in the two dose TFS treated group. For the first valid seizure onset detection in rats of the test set, in most cases (76.92% for a disjunctive combination of three detectors), detections occurred before the first MJ. According to a widely used scoring scheme for seizure-related behavioral activity [46] the first MJ is the first strong behavioral seizure manifestation. There may be other behavioral activity which includes only oral-facial movements and head nodding. After the first MJ, as the seizure develops, the amount of movement artifacts is likely to increase as rats may pass through a number of stages including multiple MJs, forelimb clonus, and severe clonic activity with rearing and falling and wild running fit. Depending on the maximum seizure stage for a particular rat the amount of movement artifacts affecting the second seizure detection may differ. Further investigation is needed to assess the percentage of second seizure detections based on tEEG power that may be attributed to movement artifacts rather than seizure-related brain activity.

B. Electrographic Seizure Activity

Results obtained for assessment of effect of TFS on power of the electrographic seizure activity using GLRT in this study are worse than the ones obtained in [30]. In this study the application of GLRT showed that TFS significantly ($p = 0.001$) reduced the power of the electrographic PTZ-induced seizure activity in the single TFS treated group (n = 5) compared to controls (n = 4) in 70% of the compared segments while in [30] significant ($p = 0.001$) reduction in the TFS treated group (n = 6) compared to controls (n = 5) occurred in more than 86% of the pairs. The major difference between these two studies is that in the current study TFS was triggered automatically while in [30] it was turned on manually after the first MJ was observed. Further investigation is needed to assess if the difference in results can be attributed to the automatic triggering of TFS or to the particularity of the current dataset.

An important limitation is the GLRT requirement of equal sizes of data segments to compare. In the current study and [30] we kept the selection of data segments consistent for control and TFS treated groups. Such time-synchronized data segmentation allows us to directly compare between corresponding groups. However, electrographic activity caused by PTZ-induced seizures is non-stationary and highly variable with periods of intense spiking activity interchanging with periods of very low activity intensities. Strict guidelines for data segment selection make the analysis vulnerable to selection partially or fully during calm periods which are less representative of the induced seizure activity. One way to reduce the effect of this nuisance factor is to use larger segments of data which in our case depends on rat survival times. A single rat expiring prematurely decreases the duration of data segments available to be compared for the whole dataset. In the future we plan to decrease the amount of PTZ administered to the rats which in turn may allow decreasing the mortality rates and increasing the duration of data segments to be compared.

We only used the electrographic seizure activity from the two dose TFS treated group for seizure onset detection analysis. However, it serves as a proof-of-principle that it is possible to close the loop with an automatic seizure control system by using noninvasive electrographic seizure activity as feedback to apply TFS or, for example, an anticonvulsant drug. Still, as can be seen in Fig. 2 the power of seizure electrographic activity reduced the furthest towards the pre-seizure baseline for the two dose TFS treated rat with no more seizure detections after the second dose of TFS (Fig. 2, panel C). Seizure electrographic activity for the single dose TFS treated rat also reduced towards baseline after the single dose of TFS but not as drastically as in the two dose TFS administration (Fig. 2, panel B). Finally, for the control rats (not treated with TFS), we expect the seizure electrographic activity to continue until PTZ diminishes so that it no longer interferes with brain activity. Unsurprisingly, the power of the seizure electrographic activity for the control rat stays high due to the continuing effect of PTZ with multiple seizure detections (Fig. 2, panel A). Further investigation is needed to study the effect of multiple doses of TFS.

C. Long-latency Behavioral Seizure Onset

As was mentioned in section 2.E. Performance metrics, there were a few rats that had long latencies to the first MJ. There was one control rat, of the 5 in the test dataset, with a latency of 9 min to the first MJ. In contrast there were 3 TFS treated rats of the 8 in the test dataset with lengthy latency to the first MJ. Two of the TFS treated rats, one with one dose the other with two; we do not have exact latencies for since they had the first MJ after we disconnected them from the instrumentation and had begun another experiment. The latencies for these two rats are approximately between 20 and 30 min. The third TFS treated rat received a single dose and had a latency of 11 min to the first MJ. In comparison the latency to the first MJ in the other rats was approximately 1.0 min. We are not certain if the

TFS was what caused the delay to the first MJ in the TFS treated rats. We need to perform more experiments to determine if TFS causes the long latency.

D. Transcranial Contacting Electrode Stimulation for Seizure Control

It was found that noninvasive electrical stimulation via ear bars captured penicillin-induced seizures in rats [47]. They applied electrical stimulation to cause seizures in hopes of controlling seizures. The electrical stimulation also caused strong tonic activity in contrast to what we observe with TFS. Cathodal tDCS, applied on the skull of rats, was found to significantly alter the threshold localized seizure activity (TLS) induced with a transcranial cortical ramp-stimulation model of focal epilepsy [48]. They found significant differences in the TLS, due to 30 minutes of tDCS applied on the cranium prior to ramp-stimulation, which lasted up to 90 minutes after stopping the tDCS. We have not tested TFS on the transcranial cortical ramp-stimulation model of focal epilepsy however we have found similar long lasting effects on PTZ-induced seizures. Previously [49] showed that TFS stopped PTZ-induced behavioral seizure activity and prevented its return. Cathodal tDCS has also been applied on the cranium after inducing pilocarpine-induced status epilepticus in immature rats [50]. In [50] they found reductions in cell loss, cognitive impairment, and frequency of convulsions. However, they do not report how they stopped the status epilepticus, whether they used an anticonvulsant or let it continue. The tDCS was applied for two consecutive weeks starting two days after the termination of status epilepticus [50]. In contrast we applied TFS for one minute on the scalp five minutes after the onset of pilocarpine-induced status epilepticus, and reapplied five minutes later if there did not appear to be a favorable response [26]. The TFS stopped or reduced electrographic and behavioral activity and was also long lasting [26]. In summary there are no direct comparisons for TFS seizure control. However, we show results that are in line with other reports.

V. Conclusion

An automatic seizure detection methodology based on a disjunctive combination of CUSUM and GLRT was validated on both sham and PTZ induced seizures in rats. These seizure deteors were part of an automated feedback seizure control system based on single or double doses of TFS administered via TCRE. An average seizure onset detection accuracy of 76.14% with sensitivity of 33.73% and specificity of 89.7% was obtained for the test set ($n = 13$). Detection of electrographic seizure activity was accomplished in advance of the early behavioral seizure activity in 76.92% of the cases. Automatically triggered TFS significantly ($p = 0.001$) reduced the electrographic seizure activity power in the single dose TFS treated group ($n = 5$) compared to controls ($n = 4$) in 70% of the paired segments further suggesting its anticonvulsant effect. While further investigation is needed to improve the methodologies proposed in this paper the preliminary results obtained in this study are promising enough to suggest the potential of a noninvasive automatic seizure control system using TCRE electrographic seizure activity as feedback. A noninvasive seizure control system is of particular importance since the majority of persons who could benefit from such a device do not want an invasive solution [51].

Acknowledgments

This research was supported in part by the National Institute of Neurological Disorders and Stroke (Award Number R21NS061335 to WGB) and NSF (award number 0643532 to YLS). The content is solely the responsibility of the authors and does not represent the official views of the National Institute of Neurological Disorders and Stroke, NIH, or the NSF.

Biographies

Oleksandr Makeyev (S'03–M'10) received his B.Sc. in mathematics and M.Sc. in statistics from Taras Shevchenko National University of Kyiv, Ukraine, in 2003 and 2005 respectively. In 2006 he began working towards his Ph.D. in engineering science from Clarkson University, Potsdam, NY receiving it in 2010. Since then he is a Postdoctoral Fellow at the Department of Electrical, Computer, and Biomedical Engineering at the University of Rhode Island, Kingston, RI. His broad research interests include development and application of computational intelligence and statistics based signal processing and pattern recognition methods to engineering problems with an emphasis on biomedical engineering.

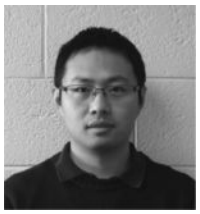

Xiang Liu (S'11) received his B. S. and M. S. degrees from the University of Science and Technology of China, Hefei, China, in 2005 and 2008, respectively. He is currently a Ph. D candidate in electrical engineering at the University of Rhode Island, Kingston, Rhode Island. His research interests are EEG sensors modeling, FPGA digital signal processing, EEG instrumentation, data acquisition system, windows driver and application software design.

Steven M. Kay is a Professor of Electrical Engineering at the University of Rhode Island, Kingston, RI and a consultant to numerous industrial concerns, and the Air Force, the Army, and the Navy. He is a Fellow of the IEEE, and he has been a distinguished lecturer for the IEEE signal processing society, associate editor for the IEEE Signal Processing Letters, and for the IEEE Transactions on Signal Processing. He has received the IEEE signal processing society education award and has recently been included on a list of the 250 most cited researchers in the world in engineering.

Yan (Lindsay) Sun received her B.S. degree with the highest honor from Peking University in 1998, and the Ph.D. degree from the University of Maryland in 2004. She joined the University of Rhode Island in 2004, where she is currently an associate professor in the department of Electrical, Computer and Biomedical Engineering. Dr. Sun's research interests include trustworthy social computing, trust management in cyber-physical systems, and information assurance. Dr. Sun is an elected member of the Information Forensics and Security Technical Committee (IFS-TC), in IEEE Signal Processing Society. She is the recipient of NSF CAREER Award.

Walter G. Besio, (S'92–M'02–SM'06) received the B.S.E.E. degree from University of Central Florida, Orlando, in 1993, and the M.S. and Ph.D. degrees in biomedical engineering from University of Miami, Coral Gables, FL, in 1997 and 2002, respectively. From 2002 to 2007, he was an Assistant Professor in the Biomedical Engineering Department, Louisiana Tech University, Ruston, LA. Since 2008 he has been in the Electrical, Computer, and Biomedical Engineering Department at the University of Rhode Island. Prior to joining academia, he worked in the medical device and electronics industries for more than 12 years. His major research interests include electrode design, Laplacian EEG, neuro-modulation, epilepsy, and brain computer interfacing. Dr. Besio's lab performs theoretical and applied research to develop novel medical devices and therapies to enhance the lives of persons with disease and disability.

References

[1]. Sander JW. The epidemiology of epilepsy revisited. Curr. Oppin. Neurol. 2003; 16(2):165–170.

[2]. Kwan P, Brodie MJ. Early identification of refractory epilepsy. N Engl J Med. 2000; 342(5):314–319. [PubMed: 10660394]

[3]. Pouratian N, Reames DL, Frysinger R, Elias WJ. Comprehensive analysis of risk factors for seizures after deep brain stimulation surgery. J Neurosurg. 2011; 115(2):310–5. [PubMed: 21548744]

[4]. Chabardes S, Kahane P, Minotti L, Koudsie A, Hirsch E, Benabid AL. Deep brain stimulation in epilepsy with particular reference to the subthalamic nucleus. Epileptic Disord. 2002; 4(Suppl 3): 83–93. [PubMed: 12105072]

[5]. Vonck K, Boon P, Achten E, De Reuck J, Caemaert J. Long-term amygdalohippocampal stimulation for refractory temporal lobe epilepsy. Ann Neurol. 2002; 52(5):556–565. [PubMed: 12402252]

[6]. Kerrigan J, Litt B, Fisher R, Cranstoun S, Frence J, Blum D, Dichter M, Shetter A, Baltuch G, Jaggi J, Krone S, Brodie M, Rise M, Graves N. Electrical stimulation of the anterior nucleus of the thalamus for the treatment of intractable epilepsy. Epilepsia. 2004; 45(4):346–354. [PubMed: 15030497]

[7]. Usui N, Maesawa S, Kajita Y, Endo O, Takebayashi S, Yoshida J. Suppression of secondary generalization of limbic seizures by stimulation of subthalamic nucleus in rats. J Neurosurgery. 2005; 102:1122–1129.

[8]. Velasco F, Carrillo-Ruiz JD, Brito F, Velasco M, Velasco AL, Marquez I, Davis R. Double-blind, randomized controlled pilot study of bilateral cerebellar stimulation for treatment of intractable motor seizures. Epilepsia. 2005; 46(7):1071–1081. [PubMed: 16026559]

[9]. Kossoff E, Ritzl E, Politsky J, Murro A, Smith J, Duckrow R, Spencer D, Bergey G. Effect of an external responsive neurostimulator on seizures and electrographic discharges during subdural electrode monitoring. Epilepsia. 2004; 45(12):1560–1567. [PubMed: 15571514]

[10]. Goodman J, Berger R, Theng T. Preemptive low-frequency stimulation decreases the incidence of amygdale-kindled seizures. Epilepsia. 2005; 46(1):1–7. [PubMed: 15660762]

[11]. Ben-Menachem E, Manon-Espaillat R, Ristanovic R, Wilder BJ, Stefan H, Mirza W, Tarver WB, Wernicke JF. Vagus nerve stimulation therapy for treatment of partial seizures, 1: a controlled study of effect on seizures. Epilepsia. 1994; 35:616–26. [PubMed: 8026408]

[12]. The vagus nerve stimulation study group. A randomized controlled trial of chronic vagus nerve stimulation for treatment of medically intractable seizures. Neurology. Feb; 1995 45(2):224–30. [PubMed: 7854516]

[13]. Handforth A, DeGiorgio C, Schachter S. Vagus nerve stimulation therapy for partial-onset seizures: a randomized active-control trial. Neurology. 1998; 51:48–55. [PubMed: 9674777]

[14]. George MS, Sackeim HA, Rush AJ, Marangell LB, Nahas Z, Husain MM, Lisanby S, Burt T, Goldman J, Ballenger JC. Vagus nerve stimulation: a new tool for brain research and therapy. Biol Psychiatry. 2000; 47(4):287–295. [PubMed: 10686263]

[15]. Patwardhan RV, Stong B, Bebin EM, Mathisen J, Grabb PA. Efficacy of vagal nerve stimulation in children with medically refractory epilepsy. Neurosurgery. 2000; 47(6):1353–1357. discussion 1357–1368. [PubMed: 11126906]

[16]. Wassermann E. Risk and safety of repetitive transcranial magnetic stimulation: report and suggested guidelines from the International Workshop on the Safety of Repetitive Transcranial Magnetic Stimulation, June 5–7, 1996. Electroencephalography and Clinical Neurophysiology. 1998; 108:1–16. [PubMed: 9474057]

[17]. Hallett M. Transcranial magnetic stimulation: a revolution in clinical neurophysiology. J Clin. Neurophysiol. 2002; 19(4):253–254. [PubMed: 12436083]

[18]. Theodore WH, Hunter K, Chen R, Vega–Bermudez F, Boroojerdi B, Reeves–Tyer P, Werhahn K, Kelley KR, Cohen L. Transcranial magnetic stimulation for the treatment of seizures: A controlled study. Neurology. 2002; 59(4):560–562. [PubMed: 12196649]

[19]. Tassinari CA, Cincotta M, Zaccara G, Michelucci R. Transcranial magnetic stimulation and epilepsy. Clinical Neurophysiology. 2003; 114:777–798. [PubMed: 12738425]

[20]. Fregni F, Thome-Souza S, Nitsche MA, Freedman SD, Valente KD, Pascual-Leone A. A controlled clinical trial of cathodal DC polarization in patients with refractory epilepsy. Epilepsia. 2006; 47(2):335–342. [PubMed: 16499758]

[21]. Theodore W, Fisher R. Brain stimulation for epilepsy. The Lancet. 2004; 3(2):111–118.

[22]. Besio W, Koka K, Aakula R, Dai W. Tri-polar concentric electrode development for high resolution EEG Laplacian electroencephalography using tri-polar concentric ring electrodes. IEEE Trans. BME. May; 2006 53(5):926–933.

[23]. Besio W, Aakula R, Koka K, Dai W, W. Development of a tri-polar concentric ring electrode for acquiring accurate Laplacian body surface potentials. Annals of Biomedical Engineering. Mar; 2006 34(3):426–435. [PubMed: 16482414]

[24]. Koka K, Besio W. Improvement of spatial selectivity and decrease of mutual information of tri-polar concentric ring electrodes. J of Neuroscience Methods. Sep.2007 165:216–222.

[25]. Wiley JD, Webster JG. Analysis and control of the current distribution under circular dispersive electrodes. IEEE Trans. BME. 1982; 29:381–385.

[26]. Besio W, Koka K, Cole A. Effects of noninvasive transcutaneous electrical stimulation via concentric ring electrodes on pilocarpine-induced status epilepticus in rats. Epilepsia. Dec; 2007 48(12):2273–2279. [PubMed: 17651415]

[27]. Besio WG, Koka K, Gale KS, Medvedev AV. Preliminary Data on Anticonvulsant Efficacy of Transcutaneous Electrical Stimulation via Novel Concentric Ring Electrodes. Epilepsy Behav. 2009; 16(1):3–46. S.C. Schachter, J.V. Guttag, S.J. Schiff, D.L. Schomer, Summit Contributors, Advances in the application of technology to epilepsy: the CIMIT/NIO Epilepsy Innovation Summit, Boston, May 2008. [PubMed: 19780225]

[28]. Sarkisian M. Overview of the current animal models for human seizure and epileptic disorders. Epilepsy & Behavior. Jun.2001 2:201–216. [PubMed: 12609365]

[29]. Besio W, Liu X, Wang L, Medvedev A, Koka K. Transcutaneous electrical stimulation via concentric ring electrodes reduced pentylenetetrazole-induced synchrony in beta and gamma bands in rats. International Journal of Neural Systems. Apr; 2011 21(2):139–149. [PubMed: 21442777]

[30]. Makeyev, O.; Liu, X.; Koka, K.; Kay, SM.; Besio, WG. Transcranial focal stimulation via concentric ring electrodes reduced power of pentylenetetrazole-induced seizure activity in rat electroencephalogram. Proceedings of 33rd Annual International Conference of the IEEE EMBS; Boston, USA. August 30 – September 3; 2011. p. 7560-7563.

[31]. Besio WG, Gale KS, Medvedev A. “Possible therapeutic effects of trancutaneous electrical stimulation via concentric ring electrodes,” Xth Workshop on Neurobiology of Epilepsy (WONOEP 2009). Epilepsia. 2010; 51(3):85–87. [PubMed: 20618408]

[32]. Besio, WG.; Liu, X.; Liu, Y.; Sun, YL.; Medvedev, AV.; Koka, K. Algorithm for automatic detection of pentylenetetrazole-induced deizures in rats. Proceedings of 33rd Annual International Conference of the IEEE EMBS; Boston, USA. August 30 – September 3; 2011. p. 8283-8286.

[33]. Besio WG, Sharma V, Spaulding J. The Effects of Concentric Ring Electrode Electrical Stimulation on Rat Skin. Annals of Biomedical Engineering. Mar; 2010 38(3):1111–1118. [PubMed: 20087776]

[34]. Mucio-Ramirez, S.; Makeyev, O.; Liu, X.; Leon-Olea, M.; Besio, W. Cortical integrity after transcutaneous focal electrical stimulation via concentric ring electrodes. Neuroscience 2011: Society for Neuroscience Annual Meeting; Washington, DC, USA. November 12–16; 2011. Program/Poster: 672.20/Y19, Online

[35]. Bragin A, Wilson CL, Fields T, Fried I, Engel J Jr. Analysis of seizure onset on the basis of wideband EEG recordings. Epilepsia. 2005; 46:59–63. [PubMed: 15987255]

[36]. Gotman J. Automatic detection of seizures and spikes. Journal of Clinical Neurophysiology. 1999; 16:130–140. [PubMed: 10359498]

[37]. Chander R, Urrestarrazu E, Gotman J. Automatic detection of high frequency oscillations in human intracerebral EEGs. Epilepsia. 2006; 47(4):37.

[38]. Paul JS, et al. Prediction of PTZ-induced seizures using wavelet-based residual entropy of cortical and subcortical field potentials. IEEE Transactions on Biomedical Engineering. 2003; 50(5):640–648. [PubMed: 12769440]

[39]. Talathi SS, et al. Non-parametric early seizure detection in an animal model of temporal lobe epilepsy. Journal of Neural Engineering. 2008; 5:85. [PubMed: 18310814]

[40]. Nandan M, Talathi SS, Myers S, Ditto WL, Khargonekar PP, Carney PR. Support vector machines for seizure detection in an animal model of chronic epilepsy. Journal of Neural Engineering. 2010; 7:036001. [PubMed: 20404397]

[41]. Philips TK, Yashchin E, Stein DM. Using statistical process control to monitor active managers. Journal of Portfolio Management. 2003; 30:86–89.

[42]. Kay, SM. Fundamentals of Statistical Signal Processing, Volume 2: Detection Theory. Prentice Hall; Upper Saddle River: 1998. ch. 6

[43]. Lehmann, EL. Testing Statistical Hypotheses. J. Wiley; New York: 1959.

[44]. Shiavi, R. Introduction to Applied Statistical Signal Analysis: Guide to Biomedical and Electrical Engineering Applications. Academic Press; Waltham: 2007. ch. 6

[45]. Alberg AJ, Park JW, Hager BW, Brock MV, Diener-West M. The use of “overall accuracy” to evaluate the validity of screening or diagnostic tests. J. Gen. Intern. Med. 2004; 19:460–465. [PubMed: 15109345]

[46]. Mirski M, Rossell L, Terry J, Fisher R. Anticonvulsant effect of anterior thalamic high frequency electrical stimulation in the rat. Epilepsy Research. Sep.1997 28:89–100. [PubMed: 9267773]

[47]. Patwardhan R, Besio W, Calvert J, Kusaka G, Kusaka I, Zhang J, Nanda A. Electroconvulsive therapy for seizure control: preliminary data in a new seizure generation and control model. Frontiers in Bioscience. 2005; 10:3013–3019. [PubMed: 15970556]

[48]. Liebetanz D, Klinker F, Hering D, Koch R, Nitsche MA, Potschka H, Löscher W, Paulus W, Tergau F. Anticonvulsant effects of transcranial direct-current stimulation (tDCS) in the rat cortical ramp model of focal epilepsy. Epilepsia. 2006; 47(7):1216–24. [PubMed: 16886986]

[49]. Besio W, Paintdakhi A, Currier R, Gale K, Medvedev A. “Reduction of pentylenetetrazole-induced seizure effects using transcutaneous electrical stimulation via concentric ring electrodes,” Proceedings of the 62nd American Epilepsy Society annual meeting. Epilepsia. 2008; 49(Suppl7):376.

[50]. Kamida T, Kong S, Eshima N, Abe T, Fujiki M, Kobayashi H. Transcranial direct current stimulation decreases convulsions and spatial memory deficits following pilocarpine-induced status epilepticus in immature rats. Behav Brain Res. 2011; 217(1):99–103. 2. [PubMed: 20826186]

[51]. Arthurs S, Zaveri HP, Frei MG, Osorio I. Patient and caregiver perspectives on seizure prediction. Epilepsy and Behavior. Nov.2010 19:474–477. [PubMed: 20851054]

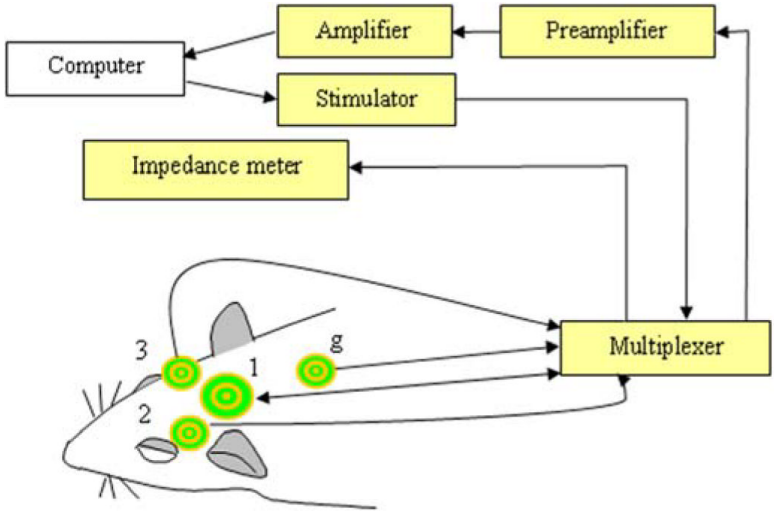

Fig. 1.

Schematic representation of the experimental setup. The TFS was applied between the outer ring and the middle disc of electrode (1). Electrodes (1), (2), and (3) were used for recording. Electrode (g) was the ground. A personal computer was used to control the system and store the data.

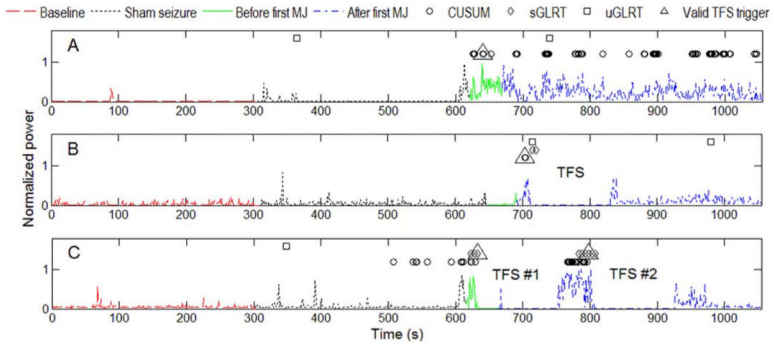

Fig. 2.

Per second normalized tEEG power and seizure detections for CUSUM, sGLRT and uGLRT detectors as well as valid TFS trigger detections for typical examples of: panel A – control rat; panel B – one dose TFS treated rat; panel C – two dose TFS treated rat.

TABLE I

Performance metrics for CUSUM, sGLRT and uGLRT detectors and their disjunctive combination.

Detector	Average			Rats with seizure onset detected prior to the first MJ (%)	Median time from PTZ injection to seizure onset detection (s)
	Accuracy (%)	Sensitivity (%)	Specificity (%)		
CUSUM	74.47	23.06	91.9	61.54	56
sGLRT	78.31	21.47	97.66	61.54	46
uGLRT	75.32	1.22	98.72	23.08	118
Disjunctive combination	76.14	33.73	89.7	76.92	18

IEEE Trans Neural Syst Rehabil Eng. Author manuscript; available in PMC 2013 July 01.